ELSEVIER

Biophysical Chemistry 57 (1995) 27–36

Biophysical Chemistry

Fluctuations and membrane heterogeneity

James R. Abney [a,b], Bethe A. Scalettar [a,*]

[a] *Department of Physics, Lewis and Clark College, Portland, OR 97219, USA*
[b] *Northwestern School of Law of Lewis and Clark College, Portland, OR 97219, USA*

Abstract

Biological membranes contain many specialized domains, ranging from tens of nanometers to several microns in size and characterized by different concentrations and compositions of protein. Because these domains influence membrane function, considerable attention has focused on understanding their origin. Here it is shown that number fluctuations and nonspecific interprotein interactions can lead to considerable heterogeneity in the distribution of membrane proteins, and to an associated submicron-scale domain structure. Number fluctuations were analyzed by modeling the membrane as a two-dimensional fluid containing interacting protein solutes. The characteristic size and lifetime of a domain in which one would expect to observe a fluctuation of specified magnitude was calculated; snapshots showing fluctuation-induced heterogeneity were generated by Monte Carlo simulation. Domain size was found to depend on the nature of the interprotein force (e.g., attractive or repulsive) and on the average protein concentration. Domain size was largest at low protein concentrations and in the presence of attractive interprotein forces, and was smallest at high protein concentrations and in the presence of repulsive interprotein forces. Domain lifetime was found to depend on domain size and on the diffusion coefficient of the proteins. In a 'typical' membrane containing 5-nm proteins with diffusion coefficient 10^{-10} cm^2/s at a density of 1000 proteins/μm^2, a 30% fluctuation will yield domains characterized by a 2-fold difference in local concentration; these domains persist over a distance of about 100 nm and have a lifetime of about 0.25 s. These results can be used to analyze the domain structure commonly observed in electron micrographs, and have implications for both number fluctuation and Monte Carlo studies of the distribution and dynamics of membrane proteins.

Keywords: Electron microscopy; Fluorescence correlation spectroscopy; Monte Carlo simulations; Membrane domains; Membrane protein; Protein–protein interactions

1. Introduction

Biological membranes are far from homogeneous mixtures of their lipid and protein components. Instead, they contain numerous specialized domains that are essential for many aspects of membrane function. For example, small (10–100 nm) scale inhomogeneities in membrane protein distribution can arise at sites of enzymatic pathways [1]. Inhomogeneities over larger (ca. 1 μm) distance scales can arise in areas where proteins aggregate to facilitate energy transduction, such as the purple membrane of *Halobacterium halobium* [2], or to facilitate cell–cell communication, such as the synapse [3,4] and the gap junction [5]. Finally, inhomogeneities over cell-wide distance scales can divide functionally polarized cells into distinct regions, such as the apical and basolateral surfaces of epithelial cells [6] and the head and tail of sperm [6,7].

* Corresponding author.

SSDI 0301-4622(95)00042-9

Because membrane heterogeneity is so important and ubiquitous, considerable effort has been directed at identifying it. Large-scale heterogeneity has been most successfully studied by combining immunolabeling techniques with light and electron microscopy [6]. Here we focus on smaller-scale membrane heterogeneity, which has been less well studied. The most direct evidence for the existence of smaller-scale nonuniformity in membrane protein distribution comes from freeze-fracture electron micrographs, which reveal that the local protein concentration in the membrane can differ significantly from the average protein concentration [8]. Biological membranes thus appear to contain many smaller-scale protein-rich and protein-poor 'domains,' which range in size from tens of nanometers to several microns.

Fluorescence techniques have also provided evidence for the existence of membrane domains. Somewhat indirect evidence comes from fluorescence recovery after photobeaching experiments in which the mobile fraction of protein and lipid was observed to depend on the size of the spot that was bleached (reviewed in Ref. [9]). This result was interpreted to mean that the membrane contains micron-sized domains that are closed to the entry or exit of protein and lipid on a time-scale of minutes. More direct evidence comes from images of fluorescently labeled cells. These frequently show micron-scale heterogeneity in fluorescence intensity, which may be a manifestation of underlying heterogeneity in protein and lipid distribution [9].

Considerable effort has also been directed at understanding the origins of membrane heterogeneity. It has been well-established that heterogeneity frequently is maintained by specific biological mechanisms, including confinement of proteins to domains created by the cytoskeleton or tight junction, attachment of proteins to the cytoskeleton, and interactions of proteins with molecules in the extracellular matrix or in the membranes of adjacent cells [6,9–13].

Membrane heterogeneity can also arise from nonspecific interactions. For example, in simple lipid bilayers, lipid–lipid interactions can cause lipid molecules to phase separate into domains of different lipid composition [14]. In simple protein/lipid membranes, protein–lipid and protein–protein interactions can cause proteins to partition preferentially into one lipid phase, creating protein-rich and protein-poor domains. Such behavior has been described theoretically in terms of phase diagrams (reviewed in Ref. [15]), which give information on the composition of phases, though not on their size. Finally, in complex biological membranes, nonspecific mechanisms can also influence heterogeneity, as has been documented in the case of the clustering of connexon proteins in the mouse liver gap junction [16,17].

In this paper, we investigate the origins of smaller-scale heterogeneity in protein distribution. We show that protein domains characterized by significantly different densities of protein will exist even within a single-phase membrane. This is a consequence of the low number density of proteins in the membrane; when number density is low, number fluctuations can become large, and the local protein density in an open area of membrane can differ significantly from the average density. We show that protein density fluctuations are influenced not just by average protein number but also by nonspecific interprotein interactions. For example, if protein molecules attract they will tend to aggregate, and their distribution will become more heterogeneous. In contrast, if protein molecules repel they will tend to disperse, and their distribution will become more homogeneous. The effects that interprotein interactions and average protein density have on both the size and lifetime of protein domains arising from number fluctuations are quantified. In addition, applications of the results to electron microscopy, number fluctuation measurements, and Monte Carlo simulations are explored.

2. Theory

2.1. Domain size

Heterogeneity in membrane protein distribution means that different regions of membrane contain different densities or compositions of protein. A variety of physical mechanisms can give rise to heterogeneity; here, we focus on number fluctuations. Specifically, consider an open region of membrane with area, A, and average protein density (protein number/unit area), ρ. In this open region, number fluctuations will cause the local protein density to differ significantly from the average density,

creating domains that are transiently enriched or depleted in protein.

One important characteristic of a domain is how much its local protein density differs from the average protein density. This difference is proportional to $N-\bar{N}$, where N and $\bar{N}=\rho A$ are the instantaneous and average number of proteins in the domain, respectively. Thus, one possible measure of heterogeneity in protein distribution is the average difference between N and $\bar{N}$, $\langle N-\bar{N}\rangle$, which is known as the first moment of the protein distribution. Unfortunately, this first moment is zero because a domain is equally likely to be enriched or depleted in protein and because on average the local and average densities do not differ [1]. It is therefore customary to characterize heterogeneity by calculating the second moment of the distribution, $\langle(N-\bar{N})^2\rangle=\overline{N^2}-\bar{N}^2$, which is not in general zero. Higher order moments can also be used to extract useful information about protein distribution [18,19], although they will not be used here.

The normalized second moment, $G(0)=(\overline{N^2}-\bar{N}^2)/\bar{N}^2$, can be used to compute the domain size corresponding to a given percent fluctuation, $\sqrt{G(0)}$, by invoking results from the thermodynamic theory of number fluctuations [20–23]. Specifically,

$$G(0)=\frac{\overline{N^2}-\bar{N}^2}{\bar{N}^2}=\frac{k_BT}{\bar{N}\left(\frac{\partial\Pi}{\partial\rho}\right)_T} \tag{1}$$

where k_B is Boltzmann's constant, T is the temperature, and Π is the osmotic pressure. It follows that

$$\bar{N}=\rho A=\frac{k_BT}{G(0)\left(\frac{\partial\Pi}{\partial\rho}\right)_T} \tag{2}$$

or

$$A=\frac{k_BT}{\rho G(0)\left(\frac{\partial\Pi}{\partial\rho}\right)_T}. \tag{3}$$

[1] This is not always the case. For example, at high concentrations, the first moment may be nonzero in a hard-disk fluid because fluctuations that would cause the local density to exceed the packing limit are prohibited.

Thus, the characteristic length, s, over which one expects to observe a percent fluctuation, $\sqrt{G(0)}$, is

$$s\sim A^{1/2}=\sqrt{\frac{k_BT}{\rho G(0)\left(\frac{\partial\Pi}{\partial\rho}\right)_T}} \tag{4}$$

The characteristic length is a function of percent fluctuation, average protein density, and the interprotein force. This lattermost dependence arises from the dependence of the isothermal osmotic compressibility, $(\partial\Pi/\partial\rho)_T$, on the interprotein force.

Expressions relating the isothermal osmotic compressibility to the interprotein force can be obtained from statistical mechanics. The most direct way to compute $(\partial\Pi/\partial\rho)_T$ is to invoke the compressibility equation, which reads [21]

$$k_BT\left(\frac{\partial\rho}{\partial\Pi}\right)_T=1+\rho\int_0^\infty[g(r)-1]2\pi r\,dr. \tag{5}$$

Here $g(r)$ is the radial distribution function, which is a measure of the probability of finding a second protein at a distance r from a given first protein [20–24]. The dependence of $(\partial\Pi/\partial\rho)_T$ on the interprotein force arises from the dependence of $g(r)$ on the force.

Unfortunately, the compressibility equation can be difficult to implement numerically because the integral is sensitive to random or systematic deviations of $g(r)$ from unity at large r. This difficulty can be overcome by first computing $\Pi(\rho)$ using less sensitive equations, and then computing the compressibility by differentiation. For a fluid containing a single solute species interacting through a pair-wise additive force, $f(r)$, the pressure can be computed from the pressure equation, which reads [24]

$$\frac{\Pi(\rho)}{k_BT}=\rho+\frac{\rho^2}{4k_BT}\int_0^\infty rf(r)\,g(r)2\pi r\,dr. \tag{6}$$

For the special case in which the particles interact through a hard-disk (excluded-volume) potential, $\Pi(\rho)$ can be computed from the Padé approximant [25]

$$\Pi(\rho)=\rho k_BT\times\left[\frac{1+0.031830f_A+0.163344f_A^2+1.943328f_A^3}{1-1.968170f_A+0.971664f_A^2}\right] \tag{7}$$

Here f_A is the area fraction occupied by the proteins, which is a function of ρ. Once $(\partial\Pi/\partial\rho)_T$ is known, domain size can be calculated from Eq. (4).

2.2. Domain lifetime

The lifetime of a domain is determined by the time required for diffusion to bring about molecular rearrangement over the distance scale of the domain. One could attempt to calculate domain lifetime very rigorously; however, a reasonable estimate can be obtained using simple arguments. Assume that proteins diffuse at a rate described by a diffusion coefficient, D. Domain lifetime, τ_c, can then be estimated using the familiar diffusion relationship, $\langle r^2 \rangle = 4Dt$ [26], by setting the mean-square displacement, $\langle r^2 \rangle$, equal to s^2, and the time equal to τ_c. This yields

$$\tau_c \sim \frac{\langle r^2 \rangle}{4D} = \frac{s^2}{4D}. \tag{8}$$

Eq. (8) shows that domain lifetime is an explicit function of domain size (i.e., the distance over which the molecules diffuse) and the speed with which the molecules diffuse. In addition, domain lifetime is an implicit function (through D) of density and the interprotein force.

3. Results

3.1. Domain size

Fluctuations in particle number give rise to domains in which the local particle concentration is transiently higher or lower than the average concentration. The characteristic size of these domains can be calculated using Eq. (4). We examined the dependence of domain size on ρ, $\sqrt{G(0)}$, and $f(r)$. Four single-solute fluids differing in protein–protein force were examined: (a) an ideal gas, in which the force is zero; (b) a hard-disk fluid, in which the force is infinite at protein–protein contact and zero elsewhere; and (c) two inverse-power-law fluids, in which the force contains soft repulsions or soft repulsions and long-range weak attractions.

Ideal gas

Domains form even in the absence of interactions. This is illustrated visually in snapshots of particle configurations, which show a marked degree of nonuniformity in the distribution of particles in an ideal gas. Fig. 1A shows snapshots at two concentrations; although particle positions are uncorrelated, regions of enhanced and diminished occupancy are still visible throughout the gas. Domain size in an ideal gas is given by

$$s \sim \frac{1}{\sqrt{\rho G(0)}} \tag{9}$$

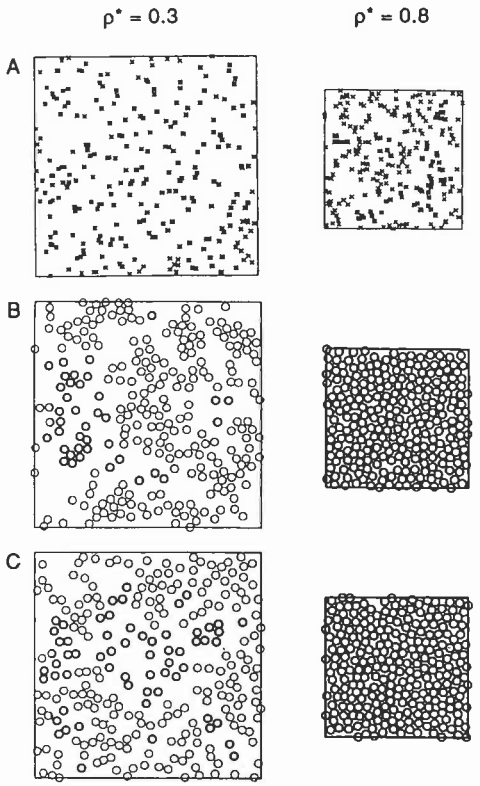

Fig. 1. Particle configurations in an ideal gas and in 4–6 inverse-power-law potential fluids. Results are shown for an (A) ideal gas and for fluids interacting through (B) an attractive-plus-repulsive 4–6 potential and (C) a purely repulsive 4–6 potential. Large panels correspond to a reduced density of 0.3, and small panels correspond to a reduced density of 0.8. Particles in the ideal gas are located at the centers of the ×'s; particles in the 4–6 fluids are located at the centers of the circles, which are drawn to radius σ. Each panel contains 256 particles. Note that fluctuations give rise to visible domains at low density, particularly in the attractive-plus-repulsive fluid. However, at high density, fluctuations and domain sizes are reduced, particularly in the 4–6 fluids.

which follows from Eq. (4) and the fact that $\Pi(\rho) = \rho k_B T$ in an ideal gas. Eq. (9) shows that domain size is inversely proportional to the square root of particle density; relatively large domains are found when ρ or $\sqrt{G(0)}$ is small. For fixed $\sqrt{G(0)}$, domain size grows as ρ falls because $\sqrt{G(0)} = 1/\sqrt{\bar{N}} = 1/\sqrt{\rho A}$. Plots of domain size in an ideal gas as a function of $\sqrt{G(0)}$ at several particle densities are shown in Figs. 2 and 3.

To develop a feel for the numbers in Figs. 2 and 3, note that a 30% fluctuation will lead to domains whose average density differs by about 2-fold, since the local particle number in the domains will then range between ca. $0.7\bar{N}$ and $1.3\bar{N}$. For an ideal gas with $\rho = 1000$ particles/μm^2, domains corresponding to a 30% fluctuation persist over a distance of ca. 100 nm.

Hard-disk fluid

Proteins in biological membranes are highly concentrated and interact with their neighbors [15,27–33]. For this reason, it is important to examine the effects of interprotein forces on domain size. The simplest interprotein force is the excluded-volume

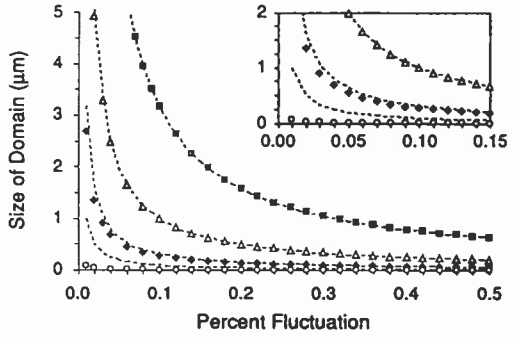

Fig. 2. Domain size in hard-disk fluids. Shown are domain sizes for 10 nm particles at four particle densities (in number/μm^2): 10 (■), 100 (△), 1000 (♦), and 10000 (○) computed using Eq. (11). The area fractions and compressibilities for these four fluids are (0.00079,1.00), (0.0079,1.03), (0.079,1.38), and (0.79,166), respectively. Also shown are domain sizes for an ideal gas (dashed line) at the same four particle densities. The ideal gas corresponds to a hard-disk fluid in which the particles have zero radius; results for the ideal gas were computed using Eq. (9). The inset shows an enlarged view of the results for small domains and percent fluctuations. Note that fluctuations cannot cause the local concentration to exceed the hard-disk packing limit, $f_A = 0.91$; this is a concern only at the highest density shown.

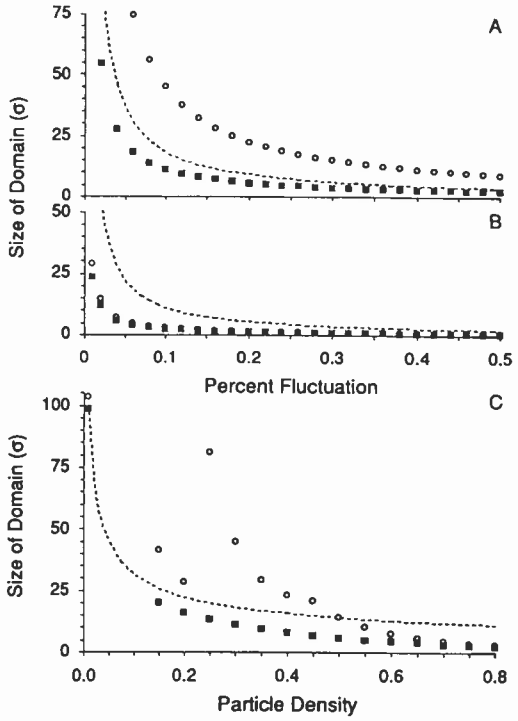

Fig. 3. Domain size in 4–6 inverse-power-law potential fluids. Results are shown for the attractive-plus-repulsive (○) and purely repulsive (■) 4–6 potentials. Also shown are results for an ideal gas (dashed line), which corresponds to the 4–6 fluids in the limit that the strength of the interaction goes to zero. Domain size versus domain composition is shown for all three systems at (A) relatively low particle density ($\rho^* = 0.3$) and (B) relatively high particle density ($\rho^* = 0.8$); these densities are the same as those of the particle configurations in Fig. 1BC. Note that domains in the purely repulsive fluid are always smaller than in the ideal gas, in qualitative agreement with the hard-disk results. In contrast, domains in the attractive-plus-repulsive fluid are larger than in the ideal gas at low densities but smaller at high densities. (C) This panel shows domain size for all three systems as a function of particle density for fixed percent fluctuation ($G(0) = 0.01$; 10% fluctuation). Results differ substantially at low concentrations but converge at high concentrations. Values for $\rho^* = 0.01$ were obtained from an analytical expression accurate at low particle densities [48]. The odd density dependence in the attractive-plus-repulsive fluid may reflect structural changes in the fluid that accompany the transition from low density (where attractions dominate) to high density (where repulsions dominate).

interaction, a strong repulsion experienced only at protein–protein contact.

$$u(r) = \begin{cases} \infty & r \le d_{HC} \\ 0 & r > d_{HC} \end{cases} \qquad (10)$$

Here $u(r)$ is the pair potential describing the interaction, and d_{HC} is the hard-disk diameter. Domain size in a hard-disk fluid can be found by differentiating the pressure in Eq. (7), and substituting the result into Eq. (4), yielding

$$s \sim \frac{1}{\sqrt{\rho G(0)}} \times \left[\frac{1 - Af_A + Bf_A^2}{\sqrt{1 + A'f_A - B'f_A^2 - C'f_A^3 - D'f_A^4 + E'f_A^5}} \right] \quad (11)$$

Here $f_A = \pi d_{HC}^2 \rho/4$, and $A = 1.968170$, $B = 0.971664$, $A' = 0.063660$, $B' = 0.544280$, $C' = 0.464128$, $D' = 0.105280$, and $E' = 0.086880$. The effects of nonidealities are contained in the bracketed term; when d_{HC}, or equivalently f_A, approaches zero, the bracketed term approaches unity and Eq. (11) reduces to the analogous ideal result, Eq. (9).

Fig. 2 shows domain size as a function of $\sqrt{G(0)}$ in the hard-disk fluid. Results are shown for a range of particle densities (10–10000 particles/μm^2) and particle sizes (0–10 nm) that spans those found in biological membranes. (Note that the 0-nm particles in fact form an ideal gas.) At low densities, the particles are relatively far apart and do not interact much; the hard-disk and ideal results are then in close agreement. However, at high densities, interactions are common and the hard-disk and ideal results differ significantly. For a given density, domain size in the hard-disk fluid is always smaller than in the ideal gas. This is because repulsive interactions cause particles to disperse, thereby suppressing fluctuations and reducing domain size. Deviations from ideality are most pronounced at high particle concentrations and at high area fractions of protein (i.e., for larger proteins) in domains whose composition differs little from the average density.

Inverse-power-law potentials

Although the hard-disk potential is an important prototype for interprotein interactions, recent evidence suggests that membrane proteins may interact through more complicated potentials [15]. These potentials may contain soft repulsions, or soft repulsions and long-range weak attractions. Domain size in the presence of such long-range interactions was analyzed using two closely related 4–6 inverse-power-law potentials. The first, containing both repulsive and attractive components, is given by

$$u(r) = \frac{27}{4} k_B T \left[(\sigma/r)^6 - (\sigma/r)^4 \right]. \quad (12)$$

Here $u(r)$ is the pair potential describing the interaction, and σ is the zero crossing for the potential. The depth of the attractive well is $k_B T$. The second, containing identical repulsions but no attractions, was obtained from Eq. (12) by a Weeks–Chandler–Andersen [34] decomposition.

$$u(r) = \begin{cases} \frac{27}{4} k_B T[(\sigma/r)^6 - (\sigma/r)^4] + k_B T & r < 1.22\sigma \\ 0 & r \geq 1.22\sigma \end{cases} \quad (13)$$

More detailed descriptions of the two potentials are given elsewhere [35].

A Padé approximant has not been determined for the two long-range 4–6 fluids. Thus, lateral pressures, $\Pi(\rho)$, were instead determined by numerical integration of Eq. (6), using radial distribution functions computed from Monte Carlo simulations [35]. Associated compressibilities were determined by numerical differentiation of the pressure using a five-point Savitzky–Golay fit [36]. Domain size was then computed by inserting the compressibility into Eq. (4).

Fig. 1B and C shows Monte Carlo-derived particle configurations for the two 4–6 fluids at relatively low and high concentrations, $\rho* = \rho\sigma^2 = 0.3$ and 0.8, respectively. At low density, particle configurations in both 4–6 fluids are distinctly nonuniform. In addition, the configurations differ significantly. In particular, attractions in the attractive-plus-repulsive fluid cause particles to tend to aggregate, leading to a visible (Fig. 1B) enhancement of number fluctuations and domain size. In contrast, at high density, particle configurations in the two fluids are similar and relatively uniform. This similarity arises because at high density particles are in close proximity, and the structure of both fluids is therefore dominated by identical repulsive interactions [37]. These structural features are also visible in the associated radial distribution functions [15].

Fig. 3A and B quantifies these observations and shows domain size as a function of $\sqrt{G(0)}$ for the two 4–6 fluids at $\rho* = 0.3$ and 0.8. For compari-

son, results for the ideal gas under otherwise identical conditions are also shown. At low concentrations, large domains are found in all three systems, although the largest domains are found in the attractive fluid and the smallest in the repulsive fluid. At high concentrations, domain size is considerably reduced. Moreover, domain size is similar in the two 4–6 fluids, and smaller than in the ideal gas.

Fig. 3C shows domain size as a function of particle density. Results are shown for $\sqrt{G(0)} = 0.1$, corresponding to 10% fluctuations in composition. Curves associated with other values of $\sqrt{G(0)}$ are identical to those shown, except for a rescaling along the vertical axis. Note that domain sizes in the purely repulsive 4–6 fluid, as in the hard-disk fluid, are always smaller than in the ideal gas. In contrast, domain size in the attractive-plus-repulsive fluid is larger than in the ideal gas for $\rho* < 0.5$ (where attractions dominate) and smaller for $\rho* > 0.5$ (where repulsions dominate). Both sets of 4–6 results converge at high particle densities.

3.2. Domain lifetime

The diffusion of membrane components underlies both the creation and dissipation of domains. Domain lifetime is therefore a function of the rate of diffusion (D) and the distance over which diffusion occurs ($s \sim \langle r^2 \rangle^{1/2}$), as described by Eq. (8). In addition, D, $\langle r^2 \rangle$, and thus the domain lifetime are implicit functions of ρ, T, and $u(r)$ (reviewed in Ref. [38]). In principle, if ρ, T, $u(r)$, and $\sqrt{G(0)}$ are known, then a value for D and the domain lifetime can be computed. However, since D and $\langle r^2 \rangle \sim s^2$ can typically be measured experimentally, it is more practical to calculate the lifetime directly from Eq. (8) using experimentally measured values for D and s. Variables such as ρ, T, and $u(r)$ will then influence domain lifetime through their effect on the measured diffusion coefficient. Note that although domains are dynamic, only the lifetime, and not the size, of the domains depends on dynamic quantities, such as the diffusion coefficient.

Fig. 4 shows domain lifetime as a function of the size of the domain. Results are shown for a range of diffusion coefficients (10^{-8}–10^{-12} cm^2/s) that spans the values observed in biological membranes

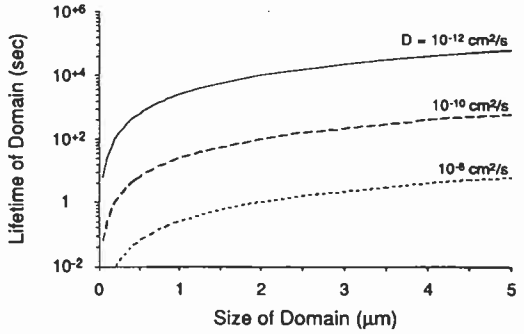

Fig. 4. Domain lifetime as a function of domain size. Results are shown for three values of the diffusion coefficient, as indicated. These values bracket those reported for proteins in membranes. These lifetimes describe the dissipation of a fluctuation of specified size, for the specified diffusion coefficient, independent of domain composition.

[39]. Domain lifetime is very sensitive to domain size, particularly for small domains. A 'typical' lifetime, computed for a small 100-nm domain with $D = 10^{-10}$ cm^2/s, is about 0.25 s. Larger domains or smaller diffusion coefficients can give rise to domain lifetimes of hundreds of seconds or more.

4. Discussion

Heterogeneity in protein distribution is a prominent and functionally significant structural feature of biological membranes. For this reason, considerable effort has been directed at identifying its origins. In many instances, heterogeneity is maintained by specific biological interactions, such as binding of protein to the cytoskeleton. However, heterogeneity can also arise in the absence of specific mechanisms. The calculations presented here show that small-scale ($\leqslant 1$ μm) heterogeneity can arise simply from number fluctuations. This is because number fluctuations in an open system are significant when average particle number is small, and micron-sized areas of the membrane contain relatively small average particle numbers, ca. 1000 proteins/μm^2.

Consider, for example, a case in which the distribution of particles in an open area A containing $\bar{N}$ particles follows Poisson statistics. The variance in the number of particles in A will then be $\bar{N}$, and the

standard deviation (square root of the variance) divided by the mean, which is $\sqrt{G(0)}$, will be [40]

$$\sqrt{G(0)} = \frac{1}{\sqrt{\bar{N}}}. \quad (14)$$

Eq. (14) is equivalent to Eq. (9) governing number fluctuations in an ideal gas and shows that one expects a 30% fluctuation in an open area containing eleven noninteracting proteins on average. Although eleven is a very small number, it is the characteristic number in a 0.1 μm × 0.1 μm area of membrane that contains 1000 proteins/μm^2, on average.

The calculations presented here also show that smaller-scale heterogeneity can be profoundly affected by interprotein interactions. In a membrane containing proteins interacting attractively through a 4–6 potential at a reduced density of 0.3, fluctuation-induced domains are about 2.5-fold larger than in the analogous ideal gas. In contrast, in a membrane containing proteins interacting repulsively at a reduced density of 0.3, fluctuation-induced domains are about 0.6-fold smaller than in the analogous ideal gas. Domain sizes predicted by an ideal gas model are accurate only for dilute membranes.

4.1. Implications for heterogeneity observed in electron micrographs

Electron micrographs of biological membranes frequently reveal considerable nonuniformity in protein distribution on the 10 nm to 1 μm distance scale [8]. Analyses of such distributions typically focus on determining whether the distributions are random and on identifying the mechanisms that lead to nonrandomness. Implicit in such analyses is an assumption that a random distribution is uniform, and that a nonuniform distribution must be maintained by nonrandom (e.g., specific) mechanisms. However, the results obtained here show that equilibrium protein distributions, which are random, can be distinctly nonuniform, especially when particle number densities are low. Indeed, number fluctuations alone can produce membrane domains that differ by a factor of two in local concentration and that persist over distances of ca. 0.1 μm. Thus, some nonuniformity in protein distributions observed in electron micrographs may arise simply from random number fluctuations. Moreover, the degree of nonuniformity in protein distribution may be profoundly influenced by the nature of the interactions between the protein molecules, as discussed above.

4.2. Implications for number fluctuation measurements

There are several techniques designed to measure number fluctuations and relate them to particle number and mobility. These include dynamic light scattering [41] and fluorescence correlation spectroscopy [42]; the latter technique has been applied to biological membranes. Experiments that follow number fluctuations often are analyzed using theories which assume that the system is behaving ideally [18,19,42–45]. Thus, expressions such as Eqs. (9) and (14) are routinely used to predict the magnitude of fluctuations in particle number in an open system.

Although solutes in dilute aqueous solutions probably do behave ideally, proteins in biological membranes do not. For example, nonideal behavior has been documented for the proteins in the gap junction, the erythrocyte membrane, and the nuclear envelope, among others (reviewed in Ref. [15]). Thus, if number fluctuation data obtained from a membrane are analyzed using a theory that is applicable to an ideal solution, the conclusions can be significantly in error. Consider, for example, a fluctuation correlation experiment in which number fluctuations are used to count particle number in an open area of membrane; this is a method of assaying for aggregation [18,19,45]. Suppose that the membrane contains proteins at 30% area fraction interacting through a hard-disk potential; a fluctuation of magnitude $\sqrt{G(0)} = 0.1$ would then arise from an area of membrane containing 26 proteins on average [Eqs. (2) and (7)]. However, if interactions are ignored, a fluctuation of magnitude 0.1 would be interpreted to arise from an area of membrane containing 100 proteins on average [Eq. (14)], leading to a 4-fold overestimate of protein number. Neglect of interactions can thus lead to significant error when number fluctuations are used to count particle number and assay for aggregation. Similar statements apply when number fluctuations are used to monitor protein dynamics [46].

4.3. Implications for Monte Carlo simulations

Recently, considerable attention has focused on numerical models of membrane behavior, including membrane organization and dynamics (reviewed in Refs. [15] and [47]). In many cases, these models are based on Monte Carlo simulations of small regions of membrane that contain on average only a few to a few thousand lipid probes or proteins. During the simulation, the number of molecules in the region is typically held constant. However, the actual number of molecules in the region should fluctuate around the average value. Quantities such as diffusion coefficients or energy transfer efficiencies computed from the simulations will therefore be in error because they will not include contributions from distributions differing in local particle density. Neglect of fluctuations is particularly significant when $\bar{N}$ is small.

Fluctuation problems can be avoided in two ways. First, simulations can be performed allowing particle number to fluctuate by using the grand canonical ensemble rather than the standard canonical ensemble. Second, results obtained from canonical-ensemble Monte Carlo simulations can be adjusted to reflect fluctuation effects by averaging results obtained at different densities against a distribution function that gives the probability of observing each of the different densities.

Acknowledgements

This paper is dedicated to Helen and Ray Abney in commemoration of their 50th wedding anniversary. This work was supported in part by a grant from the Murdock Charitable Trust (BAS) and a Dean's Fellowship for Excellence from Northwestern School of Law of Lewis and Clark College (JRA).

References

[1] H. Metzger and T. Ishizaka, Fed. Proc., 41 (1982) 7.
[2] W. Stoeckenius, R.H. Lozier and R.A. Bogomolni, Biochim. Biophys. Acta, 505 (1979) 215.
[3] S.E. Fraser and M.-m. Poo, Curr. Top. Dev. Biol., 17 (1982) 77.
[4] J.H. Steinbach and R.J. Bloch, in R.M. Gorczynski (Editor), Receptors in Cellular Recognition and Developmental Processes, Academic Press, Orlando, FL, 1986, p. 183.
[5] M.V.L. Bennett and D.C. Spray (Eds.), Gap Junctions, Cold Spring Harbor Laboratory, Cold Spring Harbor, NY, 1985.
[6] B. Gumbiner and D. Louvard, Trends Biochem. Sci., 10 (1985) 435.
[7] R.A. Cardull and D.E. Wolf, in R.A. Bloodgood (Editor), Ciliary and Flagellar Membranes, Plenum Press, NY, 1990, p. 12.
[8] S.W. Hui, in H. Plattner (Editor), Electron Microscopy of Subcellular Dynamics, CRC Press, Boca Raton, FL, 1989, p. 51.
[9] M. Edidin, Curr. Top. Membr. Transp., 36 (1990) 81.
[10] D.E. Wolf, Bioessays, 6 (1987) 116.
[11] K. Jacobson, A. Ishihara and R. Inman, Annu. Rev. Physiol., 49 (1987) 163.
[12] D. Kell, Trends Biochem. Sci., 9 (1984) 86.
[13] M.P. Sheetz, Sem. Hematol., 20 (1983) 175.
[14] M.D. Housley and K.K. Stanley, Dynamics of Biological Membranes, John Wiley and Sons, NY, 1982.
[15] J.R. Abney and B.A. Scalettar, in M.B. Jackson (Editor), Thermodynamics of Membrane Receptors and Channels, CRC Press, Boca Raton, FL, 1993, p. 183.
[16] J. Braun, J.R. Abney and J.C. Owicki, Nature, 310 (1984) 316.
[17] J.R. Abney, J. Braun and J.C. Owicki, Biophys. J., 52 (1987) 441.
[18] A.G. Palmer and N.L. Thompson, Biophys. J., 52 (1987) 257.
[19] H. Qian and E.L. Elson, Biophys. J., 57 (1990) 375.
[20] D.A. McQuarrie, Statistical Mechanics, Harper and Row, NY, 1976.
[21] H.L. Friedman, A Course in Statistical Mechanics, Prentice-Hall, NJ, 1985.
[22] T. Hill, Statistical Thermodynamics, Addison-Wesley, Reading, MA, 1960.
[23] D. Chandler, Introduction to Modern Statistical Mechanics, Oxford University Press, NY, 1987.
[24] J. Braun, J.R. Abney and J.C. Owicki, Biophys. J., 52 (1987) 427.
[25] F.H. Ree and W.G. Hoover, J. Chem. Phys., 46 (1967) 4181.
[26] H. Berg, Random Walks in Biology, Princeton University Press, Princeton, NJ, 1983.
[27] A.S. Perelson, Exp. Cell Res., 112 (1978) 309.
[28] J. Markovics, L. Glass and G.G. Maul, Exp. Cell Res., 85 (1974) 443.
[29] R.P. Pearson, S.W. Hui and T.P. Stewart, Biochim. Biophys. Acta, 557 (1979) 265.
[30] R.P. Pearson, S.I. Chan, B.A. Lewis and D.M. Engelman, Biophys. J., 43 (1983) 167.
[31] L.T. Pearson, J. Edelman and S.I. Chan, Biophys. J., 45 (1984) 863.
[32] N.D. Gershon, A. Demsey and C.W. Stackpole, Exp. Cell Res., 122 (1979) 115.
[33] T.A. Ryan, J. Meyers, D. Holowka, B. Baird and W.W. Webb, Science, 239 (1988) 61.

[34] D. Chandler, J.D. Weeks and H.C. Andersen, Science, 220 (1983) 787.
[35] J.R. Abney, B.A. Scalettar and J.C. Owicki, Biophys. J., 56 (1989) 315.
[36] A. Savitzky and M.J.E. Golay, Anal. Chem., 36 (1964) 1627.
[37] B. Widom, Science, 157 (1967) 375.
[38] B.A. Scalettar and J.R. Abney, Comm. Mol. Cell. Biophys., 7 (1991) 79.
[39] M.A. McCloskey and M.-m. Poo, J. Cell Biol., 102 (1986) 88.
[40] P.R. Bevington, Data Reduction and Error Analysis for the Physical Sciences, McGraw-Hill, NY, 1969.
[41] P.N. Pusey and R.J.A. Tough, in R. Pecora (Editor), Dynamic Light Scattering. Applications of Photon Correlation Spectroscopy, Plenum Press, NY, 1985, p. 85.
[42] E.L. Elson and D. Magde, Biopolymers, 13 (1974) 1.
[43] D. Magde, in I. Pecht and R. Rigler (Editors), Chemical Relaxation in Molecular Biology, Springer-Verlag, Berlin, 1977, p. 43.
[44] E.L. Elson and W.W. Webb, Ann. Rev. Biophys. Bioeng., 4 (1975) 311.
[45] N.O. Peterson, Biophys. J., 49 (1986) 809.
[46] J.R. Abney, B.A. Scalettar and C.R. Hackenbrock, Biophys. J., 58 (1990) 261.
[47] O.G. Mouritsen, in R. Brasseur (Editor), Molecular description of biological membrane components by computer aided conformation analysis, CRC Press, Boca Raton, FL, 1990, p. 3.
[48] B.A. Scalettar, J.R. Abney and J.C. Owicki, Proc. Natl. Acad. Sci. USA, 85 (1988) 6726.